

Exploring the chiral and deconfinement phase structure of QCD

Bernd-Jochen Schaefer

Karl-Franzens-Universität Graz, Austria

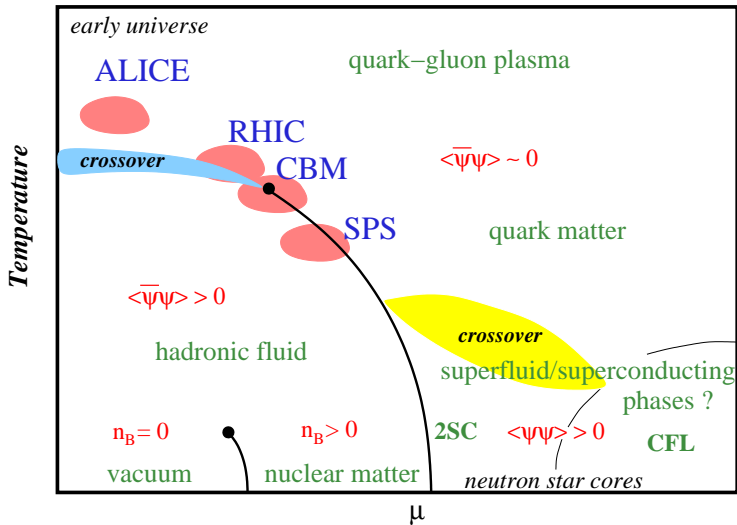


30th January, 2009

DELTA Workshop

Heidelberg, Germany

The conjectured QCD Phase Diagram



QCD Phase Transitions

QCD: two phase transitions:

- 1 restoration of chiral symmetry

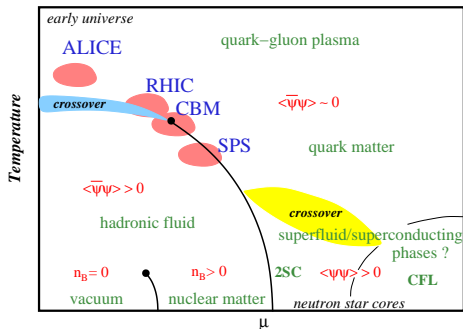
$$SU_{L+R}(N_f) \rightarrow SU_L(N_f) \times SU_R(N_f)$$

order parameter:

$$\langle \bar{q}q \rangle \begin{cases} > 0 \Leftrightarrow \text{symmetry broken, } T < T_c \\ = 0 \Leftrightarrow \text{symmetric phase, } T > T_c \end{cases}$$

associate limit: $m_q \rightarrow 0$

chiral transition: spontaneous restoration of global $SU_L(N_f) \times SU_R(N_f)$ at high T



QCD Phase Transitions

QCD: two phase transitions:

- 1 restoration of chiral symmetry
- 2 de/confinement (center symmetry)

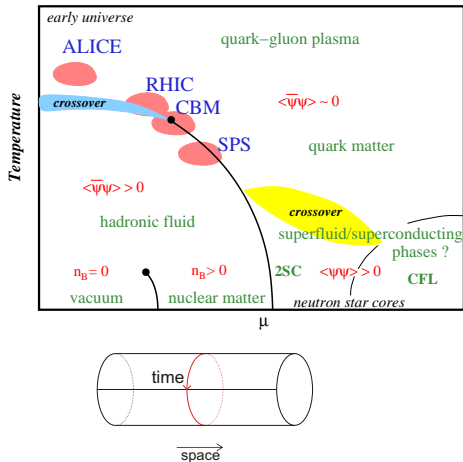
order parameter:

$$\Phi \begin{cases} = 0 \Leftrightarrow \text{confined phase, } T < T_c \\ > 0 \Leftrightarrow \text{deconfined phase, } T > T_c \end{cases}$$

$$\Phi = \frac{1}{N_c} \langle \text{tr}_c \mathcal{P} e^{i \int_0^\beta d\tau A_0(\tau, \vec{x})} \rangle$$

associate limit: $m_q \rightarrow \infty$

→ related to free energy of a static quark state: $\Phi = e^{-F_q}$

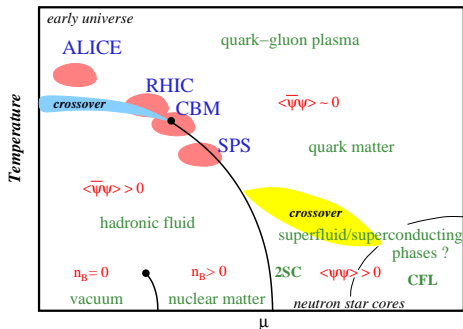


QCD Phase Transitions

QCD: two phase transitions:

- 1 restoration of chiral symmetry
- 2 de/confinement

At densities/temperatures of interest
only model calculations available



effective models:

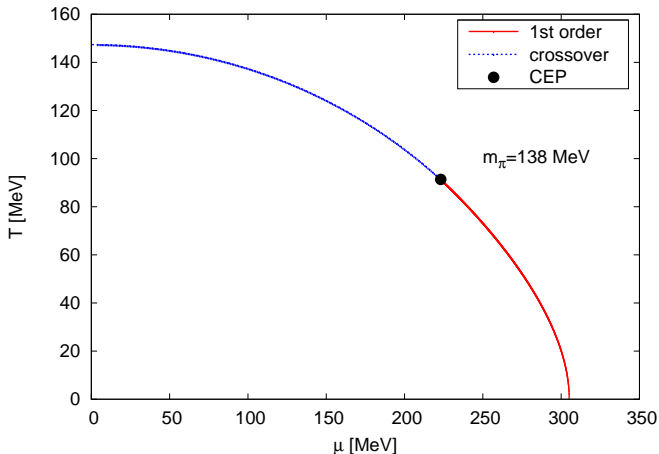
- 1 Quark-meson model or other models e.g. NJL
- 2 Polyakov-quark-meson model or PNJL models

- Two-Flavor Quark-Meson Model
 - ▷ Mean field approximation
 - ▷ Renormalization Group study
- Polyakov–Quark-Meson Model
- Three-Flavor Quark-Meson Model
- ...with Polyakov loop dynamics

- Lagrangian:

$$\mathcal{L}_{\text{qm}} = \bar{q}[i\gamma_{\mu}\partial^{\mu} - g(\sigma + i\vec{\tau}\vec{\pi}\gamma_5)]q + \frac{1}{2}(\partial_{\mu}\sigma)^2 + \frac{1}{2}(\partial_{\mu}\vec{\pi})^2 + \frac{\lambda}{4}(\sigma^2 + \vec{\pi}^2 - v^2)^2 - c\sigma$$

- Mean field analysis

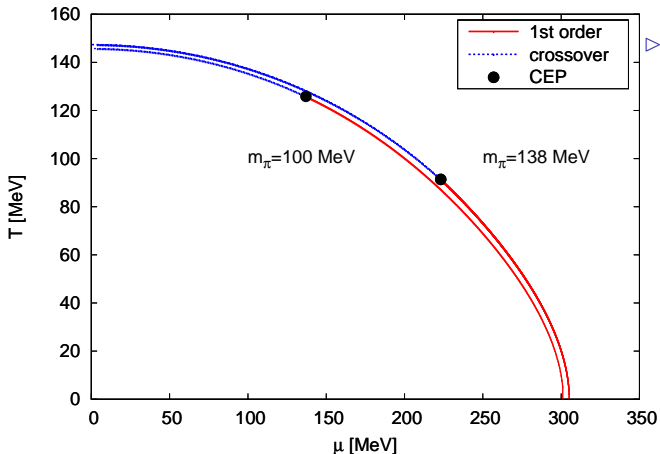


Mean field analysis

- Lagrangian:

$$\mathcal{L}_{\text{qm}} = \bar{q}[i\gamma_{\mu}\partial^{\mu} - g(\sigma + i\vec{\tau}\vec{\pi}\gamma_5)]q + \frac{1}{2}(\partial_{\mu}\sigma)^2 + \frac{1}{2}(\partial_{\mu}\vec{\pi})^2 + \frac{\lambda}{4}(\sigma^2 + \vec{\pi}^2 - v^2)^2 - c\sigma$$

- Mean field analysis



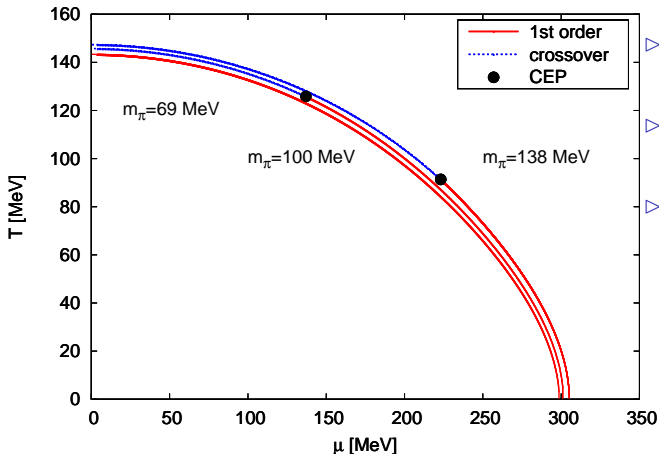
▷ as m_q decreased
CEP \rightarrow T-axis

Mean field analysis

- Lagrangian:

$$\mathcal{L}_{\text{qm}} = \bar{q}[i\gamma_{\mu}\partial^{\mu} - g(\sigma + i\vec{\tau}\vec{\pi}\gamma_5)]q + \frac{1}{2}(\partial_{\mu}\sigma)^2 + \frac{1}{2}(\partial_{\mu}\vec{\pi})^2 + \frac{\lambda}{4}(\sigma^2 + \vec{\pi}^2 - v^2)^2 - c\sigma$$

- Mean field analysis



▷ as m_q decreased
CEP \rightarrow T-axis

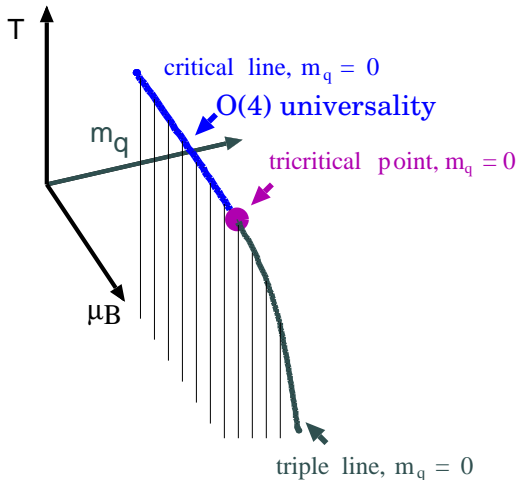
▷ chiral limit
no CEP

▷ at $\mu = 0$
 $O(4)$ scaling expected
i.e. 2nd-order PT

\rightarrow truncation effect

Phase diagram in (T, μ_B, m_q) -space

Chiral limit: $(m_q = 0)$ $SU(2) \times SU(2) \sim O(4)$ -symmetry \longrightarrow 4 modes critical $\sigma, \vec{\pi}$



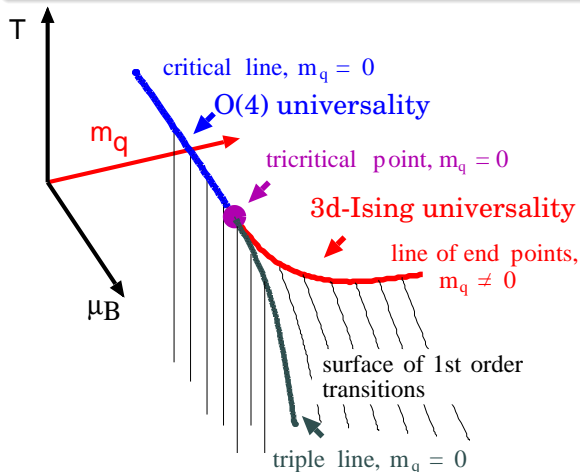
General properties

- **chiral limit**
tricritical point
(Gaussian fixed point)

Phase diagram in (T, μ_B, m_q) -space

Chiral limit: ($m_q = 0$) $SU(2) \times SU(2) \sim O(4)$ -symmetry \rightarrow 4 modes critical $\sigma, \vec{\pi}$

$m_q \neq 0$: no symmetry remains \rightarrow only one critical mode σ (Ising) ($\vec{\pi}$ massive)



General properties

- **chiral limit**
tricritical point
(Gaussian fixed point)
- **finite m_q**
critical endpoints
(3D-Ising class)

$\Gamma_k[\phi]$ scale dependent effective action ; $t = \ln(k/\Lambda)$; R_k regulators

FRG (average effective action)

[Wetterich]

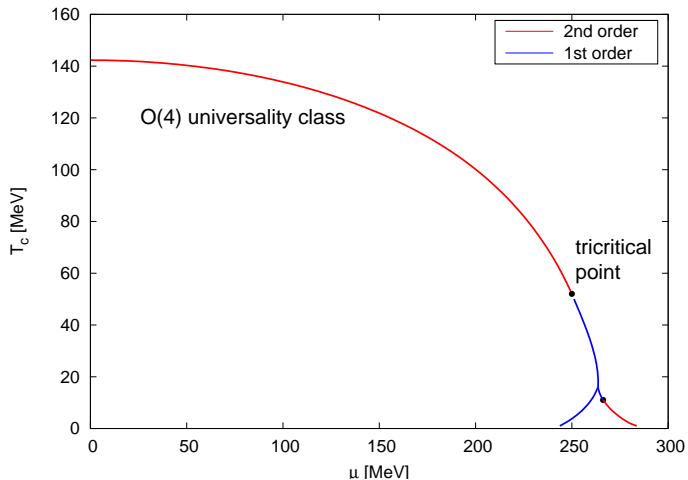
$$\partial_t \Gamma_k[\phi] = \frac{1}{2} \text{Tr} \partial_t R_k \left(\frac{1}{\Gamma_k^{(2)} + R_k} \right) ; \quad \Gamma_k^{(2)} = \frac{\delta^2 \Gamma_k}{\delta \phi \delta \phi}$$

- Ansatz for Γ_k : (LO derivative expansion \rightarrow arbitrary potential V_k)

$$\Gamma_k = \int d^4 x \bar{q} [i \gamma_\mu \partial^\mu - g(\sigma + i \vec{\tau} \cdot \vec{\pi} \gamma_5)] q + \frac{1}{2} (\partial_\mu \sigma)^2 + \frac{1}{2} (\partial_\mu \vec{\pi})^2 + V_k(\phi^2)$$

$$V_{k=\Lambda}(\phi^2) = \frac{\lambda}{4} (\sigma^2 + \vec{\pi}^2 - v^2)^2 - c \sigma$$

RG analysis:

 $O(4) \sim SU(2) \times SU(2)$ chiral limit

Chiral Phase Diagram $N_f = 2$ & $m_q \sim 280$ MeV

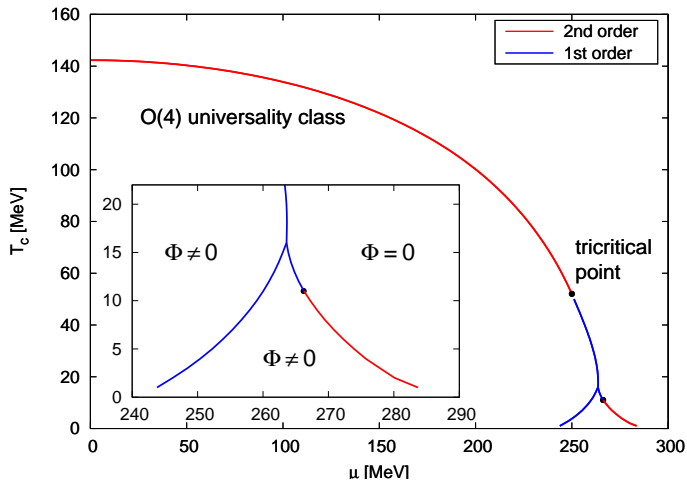
[BJS, J. Wambach, '05 & '06]

RG analysis:

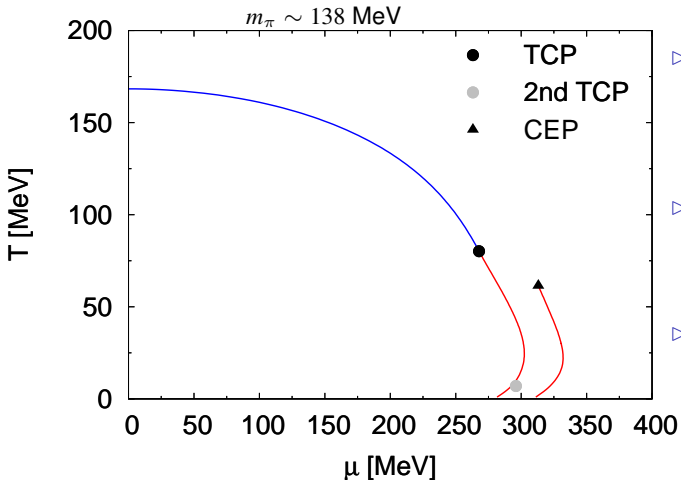
$O(4) \sim SU(2) \times SU(2)$

chiral limit

no spinodal lines!



RG Phase Diagram



▷ bending usual for RG

Clausius-Clapeyron
relation ok

▷ 2nd tricritical point

in chiral limit

▷ features

parameter independent

but locations TCP/CEP

parameter dependent

[BJS,Wambach '05 & '06]

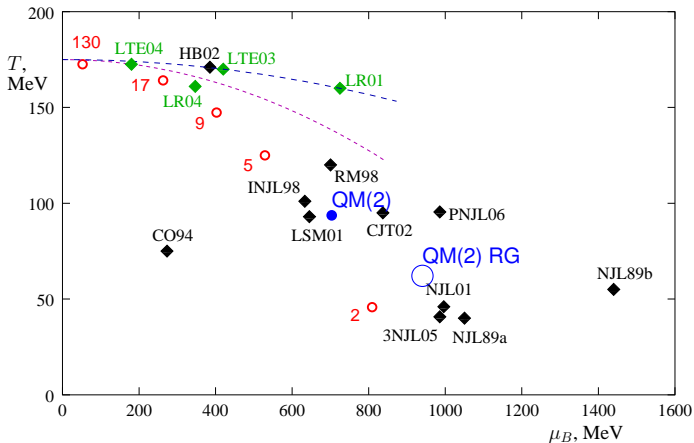
Charts of QCD Critical End Points

model studies vs. lattice simulations

Black points: models

Lines & green points: lattice

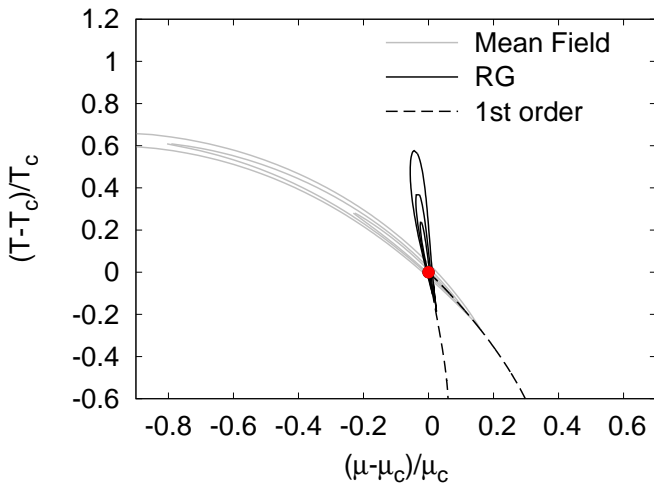
Red points: Freezeout points for HIC



lattice methods:

- reweighting
- imaginary μ_B
- Taylor expansion around $\mu_B = 0$

Stephanov '05 & '07



- Two-Flavor Quark-Meson Model
 - ▷ Mean field approximation
 - ▷ Renormalization Group study
- Polyakov–Quark-Meson Model
- Three-Flavor Quark-Meson Model
- ...with Polyakov loop dynamics

- Lagrangian $\mathcal{L}_{\text{PQM}} = \mathcal{L}_{\text{qm}} + \mathcal{L}_{\text{pol}}$ with $\mathcal{L}_{\text{pol}} = -\bar{q}\gamma_0 A_0 q - \mathcal{U}(\phi, \bar{\phi})$

1 polynomial Polyakov loop potential:

Polyakov 1978
Meisinger 1996
Pisarski 2000

$$\frac{\mathcal{U}(\phi, \bar{\phi})}{T^4} = -\frac{b_2(T, T_0)}{2} \phi \bar{\phi} - \frac{b_3}{6} (\phi^3 + \bar{\phi}^3) + \frac{b_4}{16} (\phi \bar{\phi})^2$$

with

$$b_2(T, T_0) = a_0 + a_1(T_0/T) + a_2(T_0/T)^2 + a_3(T_0/T)^3$$

- Lagrangian $\mathcal{L}_{\text{PQM}} = \mathcal{L}_{\text{qm}} + \mathcal{L}_{\text{pol}}$ with $\mathcal{L}_{\text{pol}} = -\bar{q}\gamma_0 A_0 q - \mathcal{U}(\phi, \bar{\phi})$

1 polynomial Polyakov loop potential:

Polyakov 1978

Meisinger 1996

Pisarski 2000

$$\frac{\mathcal{U}(\phi, \bar{\phi})}{T^4} = -\frac{b_2(T, T_0)}{2} \phi \bar{\phi} - \frac{b_3}{6} (\phi^3 + \bar{\phi}^3) + \frac{b_4}{16} (\phi \bar{\phi})^2$$

with

$$b_2(T, T_0) = a_0 + a_1(T_0/T) + a_2(T_0/T)^2 + a_3(T_0/T)^3$$

2 logarithmic potential:

Rössner et al. 2007

$$\frac{\mathcal{U}_{\text{log}}}{T^4} = -\frac{1}{2} a(T) \bar{\phi} \phi + b(T) \ln \left[1 - 6 \bar{\phi} \phi + 4 (\phi^3 + \bar{\phi}^3) - 3 (\bar{\phi} \phi)^2 \right]$$

with

$$a(T) = a_0 + a_1(T_0/T) + a_2(T_0/T)^2 \quad \text{and} \quad b(T) = b_3(T_0/T)^3$$

- Lagrangian $\mathcal{L}_{\text{PQM}} = \mathcal{L}_{\text{qm}} + \mathcal{L}_{\text{pol}}$ with $\mathcal{L}_{\text{pol}} = -\bar{q}\gamma_0 A_0 q - \mathcal{U}(\phi, \bar{\phi})$

1 polynomial Polyakov loop potential:

Polyakov 1978
Meisinger 1996
Pisarski 2000

$$\frac{\mathcal{U}(\phi, \bar{\phi})}{T^4} = -\frac{b_2(T, T_0)}{2} \phi \bar{\phi} - \frac{b_3}{6} (\phi^3 + \bar{\phi}^3) + \frac{b_4}{16} (\phi \bar{\phi})^2$$

with

$$b_2(T, T_0) = a_0 + a_1(T_0/T) + a_2(T_0/T)^2 + a_3(T_0/T)^3$$

3 Fukushima

Fukushima 2008

$$\mathcal{U}_{\text{Fuku}} = -bT \left\{ 54e^{-a/T} \phi \bar{\phi} + \ln \left[1 - 6\bar{\phi}\phi + 4(\phi^3 + \bar{\phi}^3) - 3(\bar{\phi}\phi)^2 \right] \right\}$$

with

a controls deconfinement b strength of mixing chiral & deconfinement

Polyakov–quark-meson (PQM) model

- Lagrangian $\mathcal{L}_{\text{PQM}} = \mathcal{L}_{\text{qm}} + \mathcal{L}_{\text{pol}}$ with $\mathcal{L}_{\text{pol}} = -\bar{q}\gamma_0 A_0 q - \mathcal{U}(\phi, \bar{\phi})$

1 polynomial Polyakov loop potential:

Polyakov 1978

Meisinger 1996

Pisarski 2000

$$\frac{\mathcal{U}(\phi, \bar{\phi})}{T^4} = -\frac{b_2(T, T_0)}{2} \phi \bar{\phi} - \frac{b_3}{6} (\phi^3 + \bar{\phi}^3) + \frac{b_4}{16} (\phi \bar{\phi})^2$$

with

$$b_2(T, T_0) = a_0 + a_1(T_0/T) + a_2(T_0/T)^2 + a_3(T_0/T)^3$$

in presence of dynamical quarks: $T_0 = T_0(N_f)$

BJS, Pawłowski, Wambach, 2007

N_f	0	1	2	2 + 1	3
T_0 [MeV]	270	240	208	187	178

Polyakov–quark-meson (PQM) model

- Lagrangian $\mathcal{L}_{\text{PQM}} = \mathcal{L}_{\text{qm}} + \mathcal{L}_{\text{pol}}$ with $\mathcal{L}_{\text{pol}} = -\bar{q}\gamma_0 A_0 q - \mathcal{U}(\phi, \bar{\phi})$

1 polynomial Polyakov loop potential:

Polyakov 1978

Meisinger 1996

Pisarski 2000

$$\frac{\mathcal{U}(\phi, \bar{\phi})}{T^4} = -\frac{b_2(T, T_0)}{2} \phi \bar{\phi} - \frac{b_3}{6} (\phi^3 + \bar{\phi}^3) + \frac{b_4}{16} (\phi \bar{\phi})^2$$

with

$$b_2(T, T_0) = a_0 + a_1(T_0/T) + a_2(T_0/T)^2 + a_3(T_0/T)^3$$

in presence of dynamical quarks: $T_0 = T_0(N_f)$

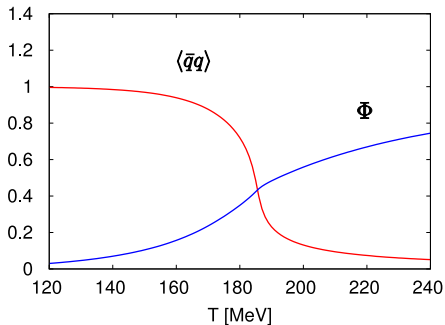
BJS, Pawłowski, Wambach, 2007

N_f	0	1	2	2 + 1	3
T_0 [MeV]	270	240	208	187	178

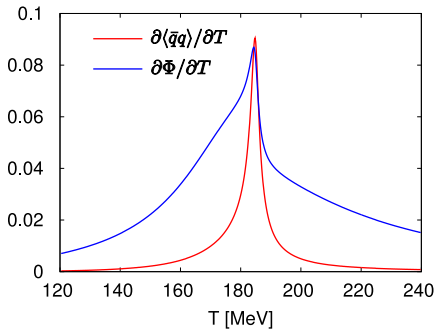
$$\mu \neq 0: \quad T_0 = T_0(N_f, \mu) \quad \bar{\phi} \neq \phi^*$$

Numerical results:

order parameters

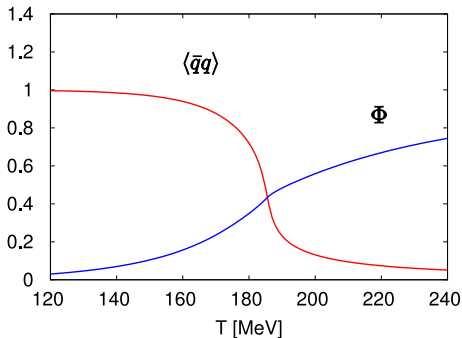


T -derivatives of order parameters

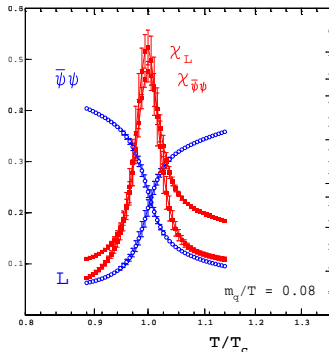


Numerical results:

order parameters



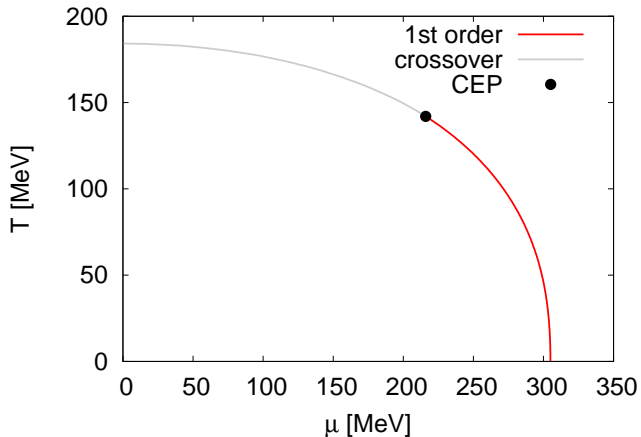
lattice



in mean field approximation

● for PQM model

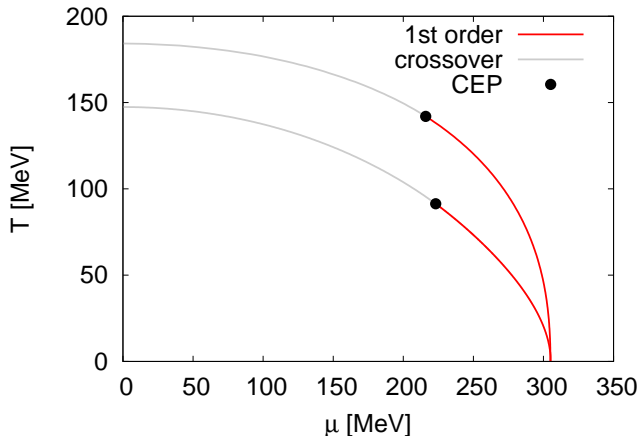
chiral transition and 'deconfinement' coincide



in mean field approximation

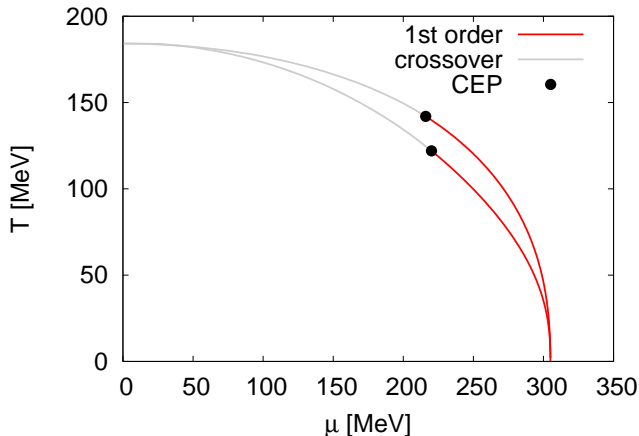
chiral transition and 'deconfinement' coincide

- for PQM model
- for QM model (lower lines)



in mean field approximation

chiral transition and 'deconfinement' coincide



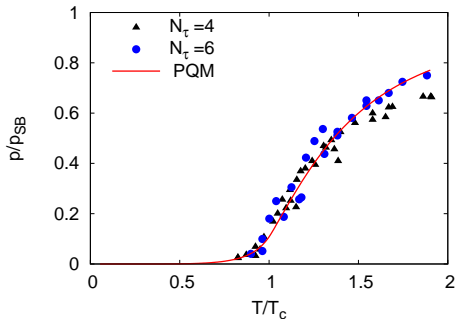
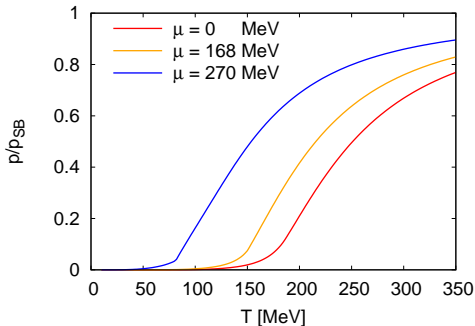
- for PQM model
- for PQM model **with** μ -modification in Polyakov loop potential (lower lines)

- perturbative pressure of QCD with N_f massless quarks

$$\frac{p}{T^4} = (N_c^2 - 1) \frac{\pi^2}{45} + N_f \left[\frac{7\pi^2}{60} + \frac{1}{2} \left(\frac{\mu}{T} \right)^2 + \frac{1}{4\pi^2} \left(\frac{\mu}{T} \right)^4 \right].$$

- $N_f = 2$:

lattice: $N_\tau = 4, 6$; $\mu = 0$



[Ali Khan et al. '01]

- Two-Flavor Quark-Meson Model
 - ▷ Mean field approximation
 - ▷ Renormalization Group study
- Polyakov–Quark-Meson Model
- Three-Flavor Quark-Meson Model
- ...with Polyakov loop dynamics

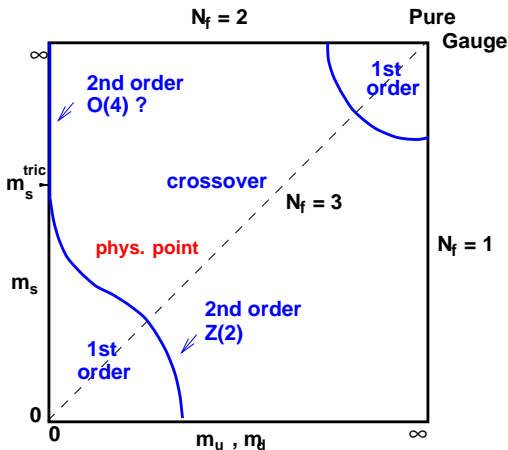
Mass Sensitivity (lattice, $N_f = 3, \mu_B = 0$)

Columbia plot:

[Brown et al. '90]

$$T_X^{N_f=2} \sim 175 \text{ MeV}$$

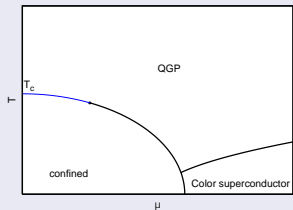
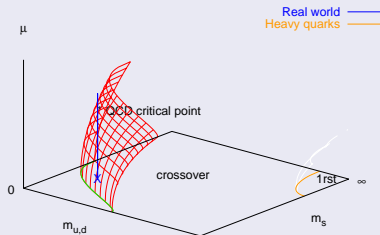
$$T_d \sim 270 \text{ MeV}$$



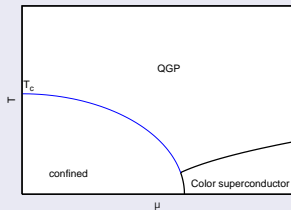
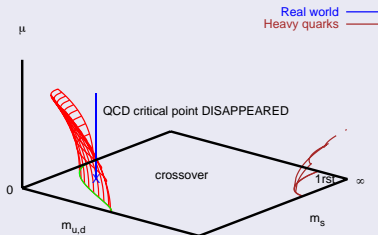
$$T_X^{N_f=3} \sim 155 \text{ MeV}$$

Mass Sensitivity (lattice, $N_f = 3, \mu_B \neq 0$)

Standard scenario: $m_c(\mu)$ increasing



Nonstandard scenario: $m_c(\mu)$ decr.



[de Forcrand, Philipsen: hep-lat/0611027]

- Lagrangian $\mathcal{L} = \mathcal{L}_{\text{quark}} + \mathcal{L}_{\text{meson}}$

$$\mathcal{L}_{\text{quark}} = \bar{q}(i\not{\partial} - g\frac{\lambda_a}{2}(\sigma_a + i\gamma_5\pi_a))q$$

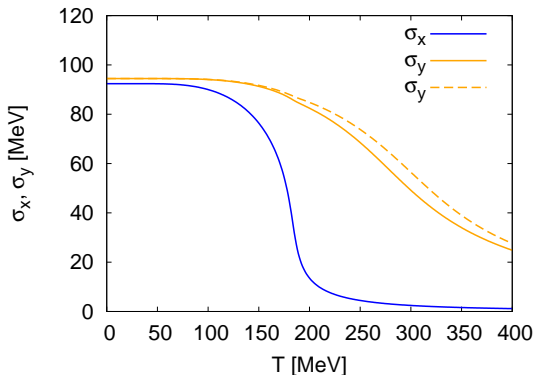
$$\begin{aligned}\mathcal{L}_{\text{meson}} = & \text{tr}(\partial_\mu\phi^\dagger\partial^\mu\phi) - m^2\text{tr}(\phi^\dagger\phi) - \lambda_1(\text{tr}(\phi^\dagger\phi))^2 \\ & - \lambda_2\text{tr}((\phi^\dagger\phi)^2) + c(\det(\phi) + \det(\phi^\dagger)) \\ & + \text{tr}H(\phi + \phi^\dagger)\end{aligned}$$

$$\text{fields: } \phi = \sum_a \frac{\lambda_a}{2}(\sigma_a + i\pi_a) \quad \text{and } H = \sum_a \frac{\lambda_a}{2}h_a$$

σ_a scalar and π_a pseudoscalar nonet

→ two condensates: nonstrange $\sigma_x(T, \mu_f)$ and strange $\sigma_y(T, \mu_f)$

with (solid) and without (dashed) $U(1)_A$ anomaly

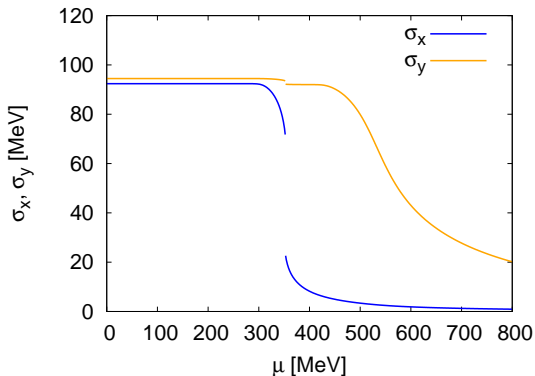


▷ almost no effect due $U(1)_A$ anomaly

▷ T_c depends on m_σ

→ two condensates: nonstrange $\sigma_x(T, \mu_f)$ and strange $\sigma_y(T, \mu_f)$

with (solid) and without (dashed) $U(1)_A$ anomaly

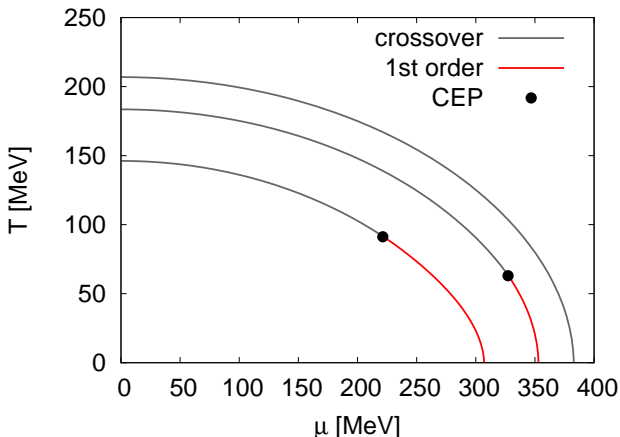


- ▷ almost no effect due $U(1)_A$ anomaly
- ▷ T_c depends on m_σ
- ▷ $\mu \equiv \mu_q = \mu_s$
- ▷ μ_c depends on m_σ

$m_\sigma = 600$ MeV (lower lines), 800 and 900 MeV

PDG: $f_0(600)$ mass=(400...1200) MeV

→ influence of existence of CEP!



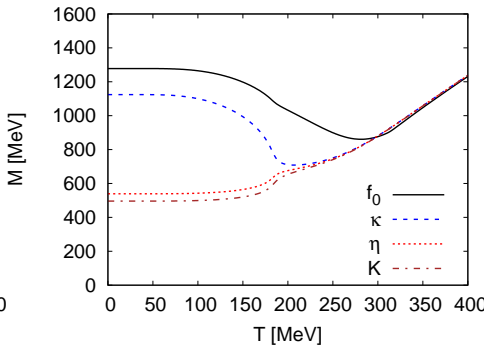
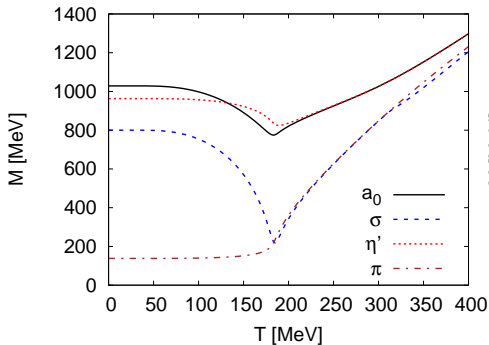
- ▷ genuine problem of linear sigma model w/o quarks at finite T
 - negative meson masses
- ▷ but not in this approximation
 - Ward identities, Goldstone theorem etc. are all valid in-medium e.g.

$$h_x = f_\pi m_\pi^2$$

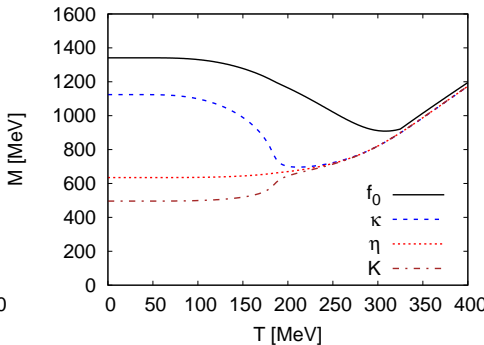
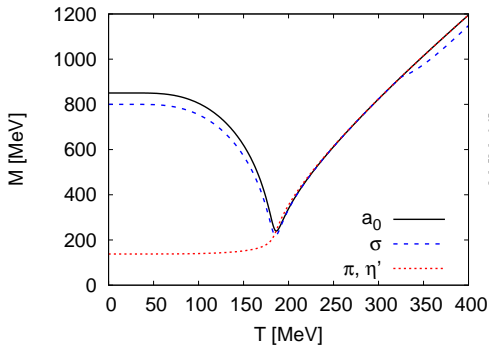
similar in strange sector

- ▷ At low temperatures: mesons dominate
- At high temperatures: quarks dominate

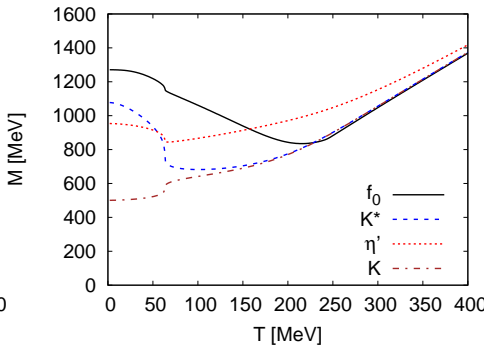
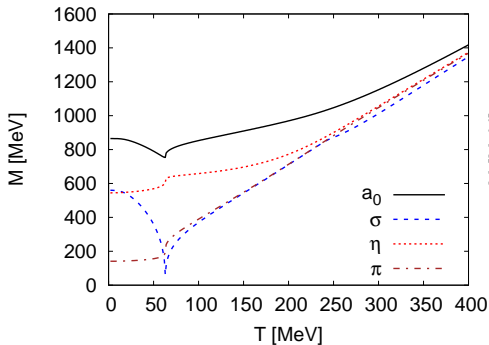
masses with $U(1)_A$ anomaly



masses without $U(1)_A$ anomaly



masses with $U(1)_A$ anomaly

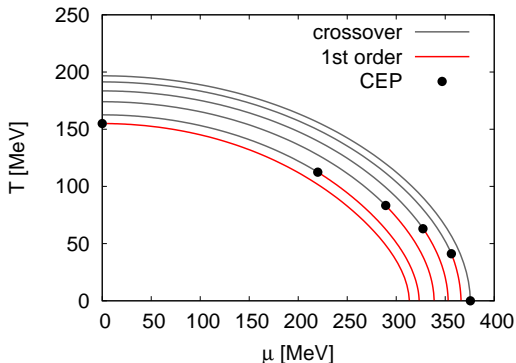


Mass sensitivity

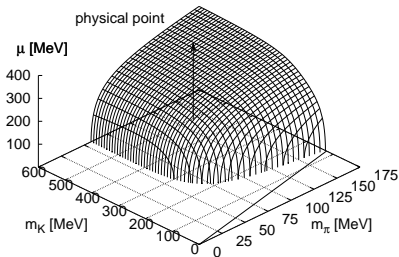
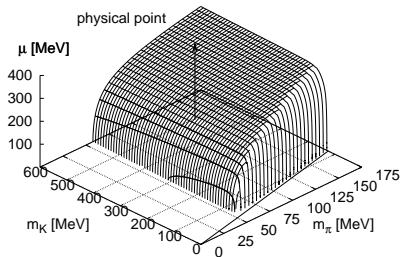
RG arguments predict for $N_f = 3$ 1st-order in chiral limit

▷ $m_\pi/m_\pi^* = 0.49$ (lower line), 0.6, 0.8 . . . , 1.36 (upper line) $m_\pi^* = 138$ MeV

with $U(1)_A$, $m_\sigma = 800$ MeV



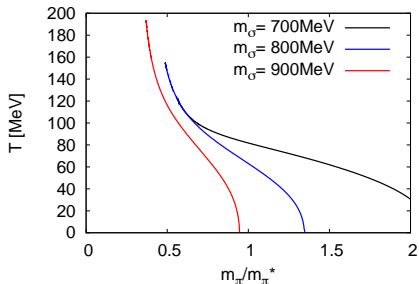
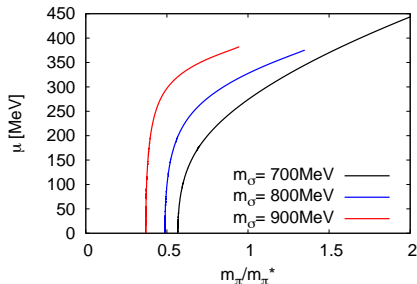
- chiral critical surface in (m_π, m_K) plane

with $U(1)_A$ without $U(1)_A$ 

- chiral critical surface in (m_π, m_K) plane

→ cuts along fixed m_π/m_K ratio through physical point

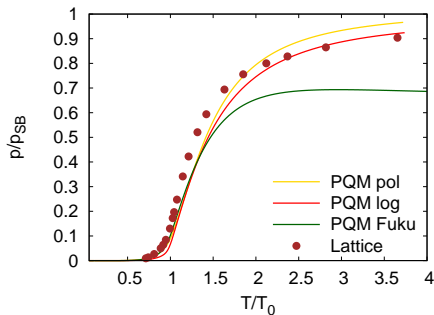
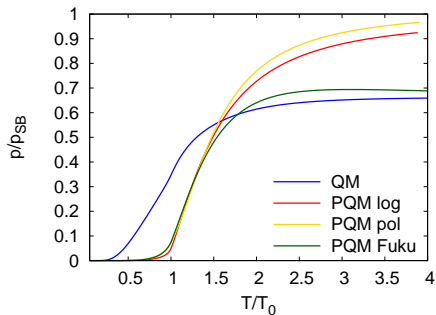
$m_\pi^* = 138 \text{ MeV}$, $m_K^* = 496 \text{ MeV}$ (physical point)

critical T_c critical μ 

- Two-Flavor Quark-Meson Model
 - ▷ Mean field approximation
 - ▷ Renormalization Group study
- Polyakov–Quark-Meson Model
- Three-Flavor Quark-Meson Model
- ...with Polyakov loop dynamics

[BJS, M. Wagner; to be published '08]

$$\text{SB limit: } \frac{p_{\text{SB}}}{T^4} = 2(N_c^2 - 1) \frac{\pi^2}{90} + N_f N_c \frac{7\pi^2}{180}$$

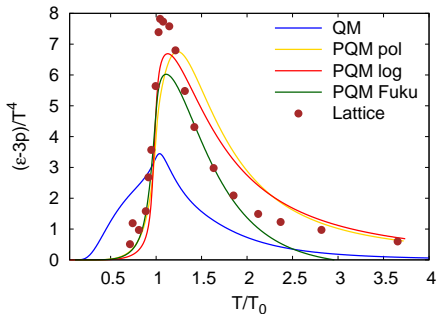
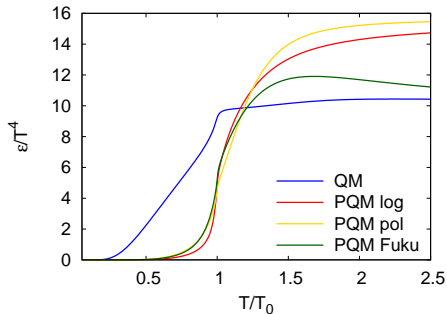


$m_\pi \sim 220 \text{ MeV}$

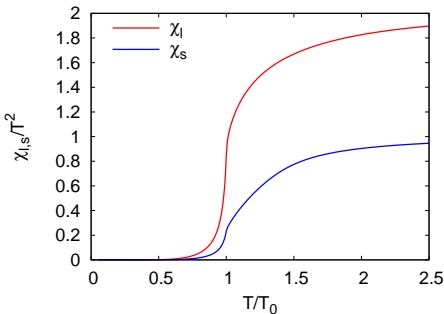
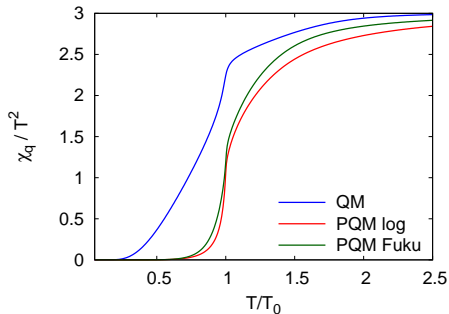
$N_\tau = 8$

[Cheng et al. '08]

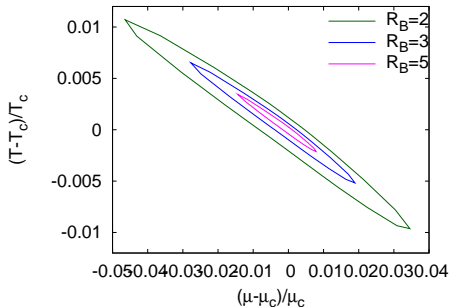
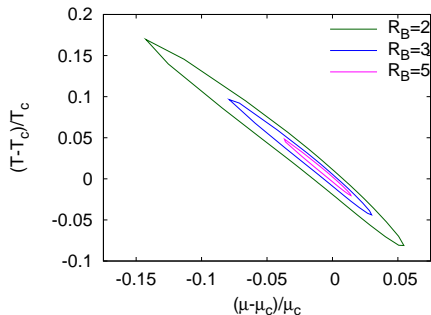
$$\text{SB limit: } \frac{P_{\text{SB}}}{T^4} = 2(N_c^2 - 1) \frac{\pi^2}{90} + N_f N_c \frac{7\pi^2}{180}$$



SB limit:
$$\frac{P_{SB}}{T^4} = 2(N_c^2 - 1) \frac{\pi^2}{90} + N_f N_c \frac{7\pi^2}{180}$$



size of the critical region:



Taylor expansion:

$$\frac{p(T, \mu)}{T^4} = \sum_{n=0}^{\infty} c_n(T) \left(\frac{\mu}{T}\right)^n \quad \text{with} \quad c_n(T) = \frac{1}{n!} \left. \frac{\partial^n (p(T, \mu)/T^4)}{\partial (\mu/T)^n} \right|_{\mu=0}$$

high temperature limits:

$$c_0(T \rightarrow \infty) = \frac{7N_c N_f \pi^2}{180},$$

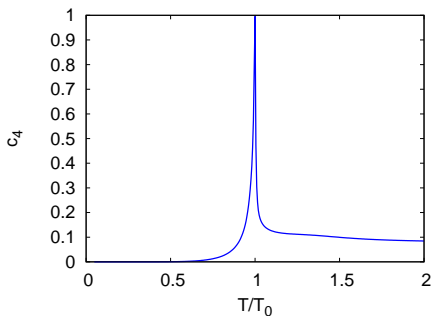
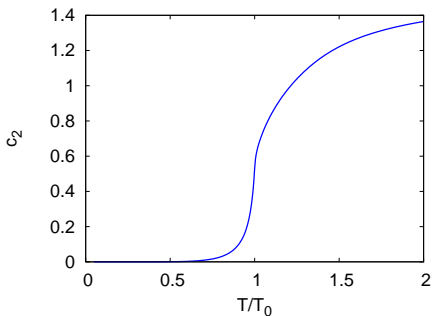
$$c_2(T \rightarrow \infty) = \frac{N_c N_f}{6},$$

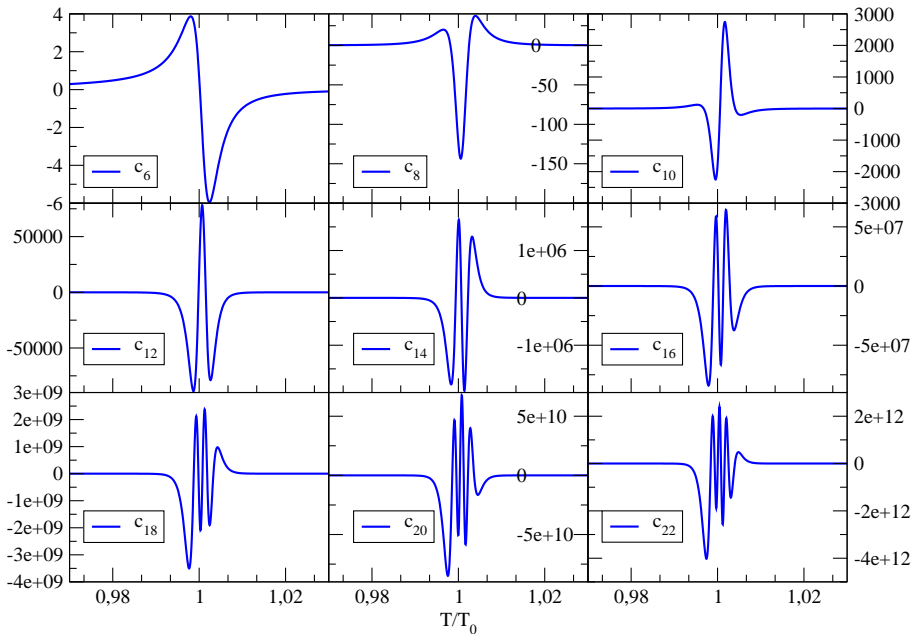
$$c_4(T \rightarrow \infty) = \frac{N_c N_f}{12\pi^2}$$

$$c_n(T \rightarrow \infty) = 0 \text{ for } n > 4.$$

Taylor expansion:

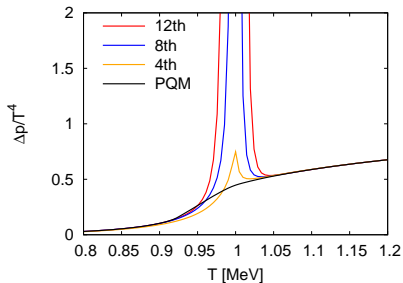
$$\frac{p(T, \mu)}{T^4} = \sum_{n=0}^{\infty} c_n(T) \left(\frac{\mu}{T}\right)^n \quad \text{with} \quad c_n(T) = \frac{1}{n!} \left. \frac{\partial^n (p(T, \mu)/T^4)}{\partial (\mu/T)^n} \right|_{\mu=0}$$

first three coefficients: c_0 : pressure $\mu = 0$ 

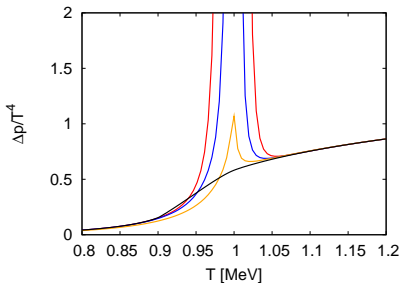


Finite density extrapolations $N_f = 2 + 1$ PQM

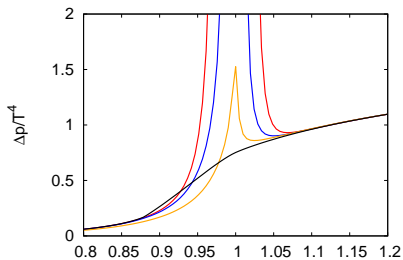
$\mu/T = 0.8$



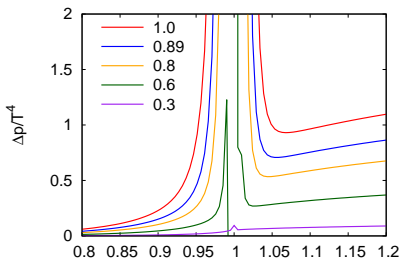
$\mu/T = \mu_c/T_c$



$\mu/T = 1.$

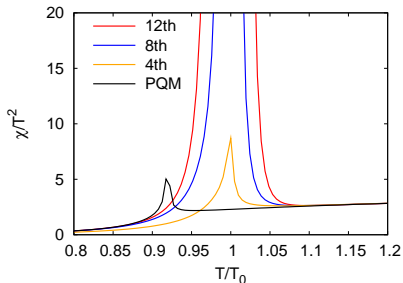


up to $n = 12$

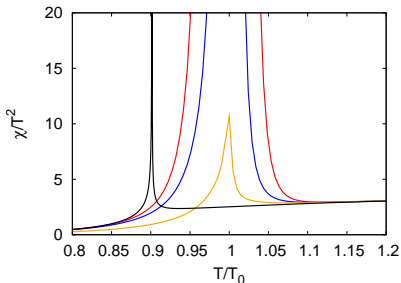


Finite density extrapolations $N_f = 2 + 1$ PQM

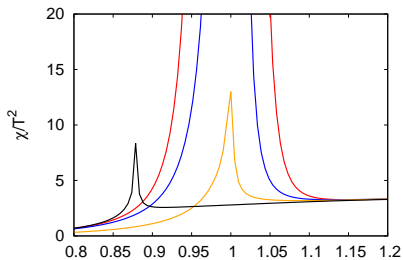
$\mu/T = 0.8$



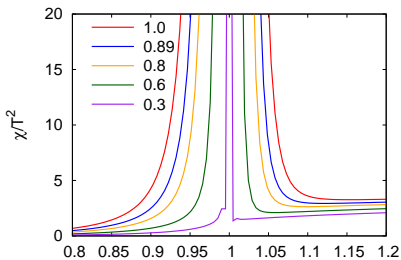
$\mu/T = \mu_c/T_c$



$\mu/T = 1.$



up to $n = 12$



Quark-meson model study for $N_F = 2$

→ Mean field versus RG

Influence of fluctuations on phase diagram

Findings:

- ▷ MF phase diagram: no TCP (in chiral limit) found
- ▷ RG phase diagram: two TCP's (in chiral limit) & CEP found
- ▷ Size of critical region via susceptibilities: “compressed” with fluctuations

Quark-meson model study for $N_F = 3$

→ Mean-field approximation

no need for Optimized Perturbation Theory

with and without axial anomaly

Polyakov–quark-meson model study for $N_F = 2$

→ mean-field approximation

Findings:

- ▷ Parameter in Polyakov loop potential: $T_0 \Rightarrow T_0(N_f, \mu)$

pure gauge: $T_0 \sim 270$ MeV

$N_f = 2$: $T_0 \sim 210$ MeV

- ▷ Chiral & deconfinement transition **coincide**

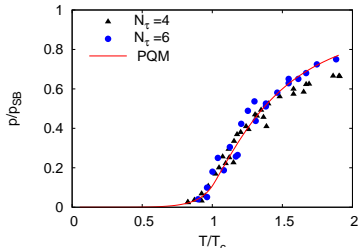
- ▷ Mean-field approximation encouraging

Quark-meson model is renormalizable

→ no UV cutoff parameter (cf. PNJL model)

- ▷ Taylorcoefficient $c_n(T) \rightarrow$ high order

- ▷ useful to develop general arguments to determine CEP location



- ▶ include quark-meson dynamics in PQM model and for $N_f = 3$ with FRG
- ▶ include glue dynamics with FRG \rightarrow full QCD
(step by step)